Quantification of Cu and Zn in antifouling paint films by XRF

Talanta xxx (xxxx) xxx

Contents lists available at ScienceDirect

Talanta

journal homepage: www.elsevier.com/locate/talanta

Quantification of Cu and Zn in antifouling paint films by XRF

Lagerström Maria *, Ytreberg Erik **

Department of Mechanics and Maritime Sciences, Chalmers University of Technology, SE 412 96, Gothenburg, Sweden

ARTICLE INFO

Keywords:
Antifouling paint
XRF
Release rate
Leaching rate
Copper
Zinc

ABSTRACT

Methods to determine the release of biocides (e.g. copper) and substances of concern (e.g. zinc) from antifouling paints are required for both the development of efficient products and their environmental risk assessment. To date, there are only two standardized methods available to estimate such release rates, but their reliability has been put into question. An alternative method, allowing determination of environmental release rates in the field of metallic or organometallic biocides by X-Ray Fluorescence (XRF), has been developed and applied in recent years. In this study, the potential for standardization of the XRF method is investigated through evaluation of its accuracy, precision and transferability between instruments. Accurate quantification of copper (Cu) and zinc (Zn) in μg cm^{-2}, despite differences in chemical composition, was demonstrated through comparison of calibration regression slopes for ten different antifouling paints and confirmed through the measurement of validation samples. Universal antifouling paint calibration curves are proposed for the determination of Cu and Zn in thin paint films, with a prediction uncertainty of around ±130 μg/cm^2 for both metals. The transferability of the method to another instrument was also demonstrated. For both analyzers, concentrations of validation samples were within 5% of those determined through wet chemical analysis. Pre-requisites and recommendations for the application of the method as well as its applicability to both short- and long-term release rate studies in the field are also presented and discussed.

Credit author statement

Maria Lagerström: Conceptualization, Methodology, Software, Validation, Formal analysis, Investigation, Data curation, Writing - original draft, Visualization, Supervision. Erik Ytreberg: Conceptualization, Methodology, Investigation, Writing - review & editing, Supervision, Funding acquisition.

1. Introduction

Antifouling paints are applied on vessel hulls to prevent marine biofouling (e.g. algae, barnacles and mussels) [1]. The colonization of marine organisms on the hull surface will otherwise lead to reduced speed and increased fuel consumption [2]. The release of active substances, i.e. toxic biocides, from the coating act to repel and/or poison fouling organisms [3]. Although a variety of biocides have been used throughout history, copper compounds and mainly cuprous oxide (Cu_2O), have by far been the dominant active substances in antifouling paints since the phase out of tributyltin (TBT) in antifouling coatings [4, 5]. A content of 30–40 wt % Cu_2O (ww) is typical in antifouling coatings, making Cu one of the major constituents of the paint films [6]. Another commonly added metallic compound is zinc oxide (ZnO), typically in the range of 10–25 wt % [7]. According to the European Council of the Paint, Printing Ink and Artists' Colors Industry (CEPE), the function of ZnO in antifouling paints is to regulate the dissolution of the paint film, stabilize the wet paint in the can, protect the dry film from UV damage and act as a pigment (whitener) [8]. In the EU, ZnO is hence not classified as a biocide but considered to be a Substance of Concern (SoC), i.e. a co-formulant in a biocidal product with an inherent capacity to cause an adverse effect on humans, animals or the environment [9]. Upon immersion, the soluble pigment particles of Cu_2O and ZnO in the paint film are dissolved, resulting in a release of Cu and Zn [10].

Knowledge of the release rate of biocides from antifouling paints is required to ensure that the product will be effective in preventing fouling, i.e. that the release rate of biocides is sufficient [3]. Release rates of biocides and SoCs are also required in the risk assessment procedure of antifouling coatings in order to predict environmental concentrations and potential impacts on the marine environment [11–13].

* Corresponding author.
** Corresponding author.
E-mail addresses: maria.lagerstrom@chalmers.se (L. Maria), erik.ytreberg@chalmers.se (Y. Erik).

https://doi.org/10.1016/j.talanta.2020.121820
Received 25 September 2020; Received in revised form 23 October 2020; Accepted 26 October 2020
Available online 28 October 2020

To date, there are only two standardized methods for estimating the biocidal release rate from antifouling paints: a laboratory rotating cylinder method and a mass balance calculation method [14]. Both are have been shown to poorly predict environmental releases of biocides [7] and corrections factors have been proposed to account for potential discrepancies (Finnie, 2006). An alternative method, allowing for determination of environmental release rates in the field of metallic or organometallic biocides by X-Ray Fluorescence (XRF), has been developed and applied in recent years [7,15]. XRF is highly suitable for the measurement of metals in antifouling paint films. It is commonly used for non-destructive analysis of metals in solid samples and an application for measuring lead in indoor paints was developed already in the 1990's [16]. For release rate measurements, the metal area concentration (in $\mu g/cm^2$) in thin paint films coated on panels is determined by XRF before the panels are exposed in the field, e.g. in a marina or attached to a vessel hull. The panels are retrieved after an immersion period of weeks to months and reanalyzed. The calculated difference in area concentration represents the amount of metal released from the paint over the given immersion period and a release rate (in $\mu g\ cm^{-2}\ d^{-1}$) can thus be inferred. The principles, advantages and drawbacks of the three release rate methods are summarized in Table SI1. The XRF analysis method holds several advantages over the currently standardized methods, the overriding one being its ability to determine environmentally relevant release rates, i.e. the release rates occurring when the paint is exposed to field conditions.

During XRF analysis, primary X-rays excite the atoms in the sample which then emit secondary X-rays at energies characteristic to the specific elements present. The secondary X-rays are detected by the instrument, yielding a spectra where the intensity of the signal at the characteristic energy of a given element, typically measured as peak area, is proportional to the concentration of that element in the sample [17]. The analysis is quick, typically seconds to minutes, and the instrumentation relatively cheap, especially when it comes to portable/handheld units (around $30,000) [18,19]. Accurate analysis requires however specific calibration and there are also requirements on the physical characteristics of the sample. For XRF analysis of thin films, sample thickness is an important characteristic. As the depth of analysis is not unlimited, sample thickness must be controlled for accurate measurement of Cu and Zn in antifouling paint films. The intensity of the XRF signal, i.e. the analyte peak area, will only increase linearly with sample thickness up to a certain threshold beyond which the X-Rays are subject to absorption attenuation by the sample [20] (Fig. 1a). This threshold is known as the critical thickness, d_{thin}, and its magnitude will depend on the element of interest as well as the properties of the matrix [21]. At thicknesses beyond the d_{thin} of an element, the full amount of that element present within the paint film will no longer be detected and quantified due to signal attenuation. The effect of increased thickness on the detected signal (in counts per second) was studied for two antifouling paints of different compositions in Ytreberg et al., 2017. For Cu and Zn, d_{thin} was found to be around 40 μm and 52 μm for each of the two paints. A general recommendation of a dry film thickness (DFT) $\leq$ 40 μm was therefore suggested for quantitative measurements of antifouling paint thin films. If this recommended DFT is exceeded, the concentration of Cu and Zn in the paint film may be underestimated.

In addition to thickness, sample composition will also influence the measurement. XRF analysis is a matrix-dependent technique as the intensity of an analyte's peak will depend not only on its own concentration, but also of those of the other elements making up the sample [18]. Quantification methods by XRF are therefore subject to errors by two types of matrix effects: absorption and enhancement (Fig. 1b). Thus, for quantitative analysis, care must be taken to minimize and/or correct for any such effects. For the analysis of thin films, absorption/enhancement effects are reduced or even avoided at thicknesses $<$ d_{thin} [17,22]. Additionally, the choice of quantification method can aid in reducing biased results due to matrix effects. Depending on the application, XRF quantification can be carried out using either empirical or theoretical methods. The latter involves calibration using pure element as standards and mathematical models to derive analyte concentrations [23]. With the empirical method, on the other hand, a custom calibration curve is established based on standards with chemical and physical properties similar to those of unknown samples [24]. The preparation of the calibration standards is the critical step in the calibration process. Although the applicability of the empirical method is limited to a certain type of sample and concentration range, it allows for higher accuracy as the risk of biased results due to matrix effects is reduced or avoided [25]. To this end, the XRF antifouling paint calibration in Lagerström et al., 2018 was established from standards prepared through addition of Cu_2O and ZnO to a generic antifouling paint base. However, apart from differences in Cu and Zn concentrations, variations in other elements in the paint could potentially result in differences in absorptive properties between antifouling paint products. Specifically, the concentrations of compounds acting as fillers/extenders (e.g. barium sulphate, calcium carbonate, etc) as well as the color pigments added (e.g. iron oxide, titanium oxide, etc) may vary between paints [5,26]. Complementary compensation methods involving internal standardization using scattered X-Rays, also known as scatter

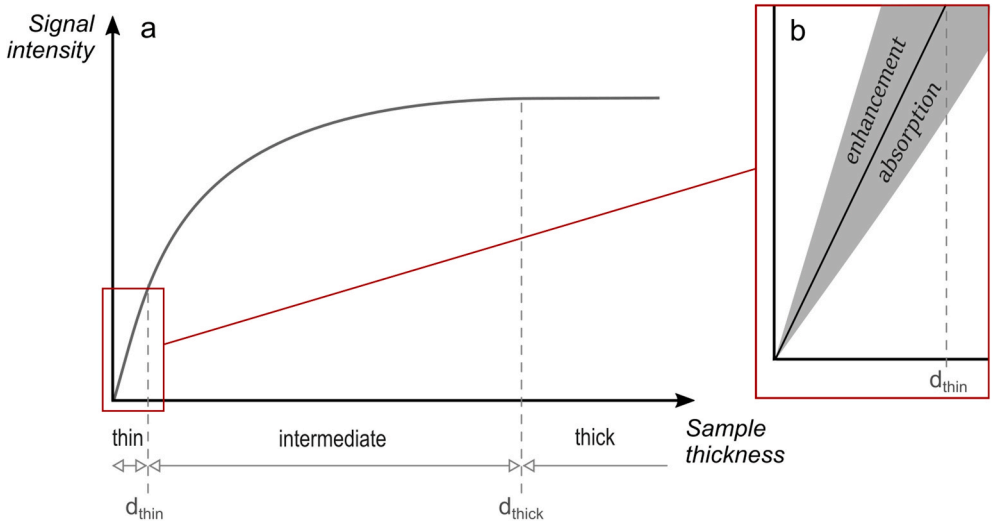

Fig. 1. Schematic of the effect of sample thickness (and by default analyte concentration in a homogenous sample) on the XRF signal intensity (i.e. the area) of an element peak (a). The effect of potential enhancement or absorption on the slope of the linear range is also illustrated (b).

methods, may however be useful here. Upon irradiation of a sample, backscattering of X-ray radiation from the excitation source will result in both a continuous background scatter (the continuum) as well as coherent (Rayleigh) and incoherent (Compton) scatter peaks of the X-Ray tube anode element [17]. These scatter artifacts are present in the spectrum of every sample. As the scattered radiation undergoes matrix absorption similar to that of analyte peaks, quantification carried out based on their ratio will be less sensitive to variations in sample composition [23]. Scatter methods are however not generally effective against enhancement effects [17]. The background-ratio method, whereby peak areas are ratioed to a section of the continuum scatter, has been applied to all measurements in the authors' previous publications where XRF analysis of antifouling paint films has been utilized [7,15], but whether this is sufficient to correct for potential differences in absorptive properties between antifouling coatings has not been thoroughly investigated.

Demonstrating accurate quantification despite differences in chemical composition between antifouling paints as well as good agreement of results produced on different XRF instruments is a prerequisite for the XRF analysis of antifouling paint films to be standardized. The aim of this study was thus to examine if and to what extent variations in paint formulation, i.e. differences in absorptive properties, affect the accuracy of the XRF quantification. For this purpose, ten antifouling paints, holding a wide range of Cu and Zn concentrations as well as different pigments and fillers, were selected to compare the relationship between the concentrations of Cu and Zn and their respective Kα peak intensities. Additionally, measurements were performed on different XRF-instruments and with different types of panel materials to assess the performance and transferability of the method.

2. Materials & methods

2.1. Antifouling paints

In total, 20 commercial antifouling paints and one primer paint were analyzed to investigate the variability in element composition of antifouling paints on the market (Table 1). Paints from four different manufacturers and of four main colors (black, red, blue and white) were investigated. Most of the paints (P1 – P17, P19 and P20) were antifouling paints containing Cu_2O as the main biocide. P18 was an antifouling paint for use in freshwater which does not contain Cu and is therefore not classified as a biocidal product. Furthermore, a primer (P21) was also analyzed. The antifouling coatings were selected to obtain a wide range of Cu_2O, and hence most of the antifouling paints are for amateur use (n = 18) and only two coatings are for professional use.

The chemical analysis was performed by ALS Scandinavia AB and two different extraction methods were used on samples of dried paint. Aliquots of paint were poured off, left to dry in petri dishes and scraped to produce paint flakes samples for the analyses. For each paint, one subsample was subjected to microwave assisted digestion with a hydrofluoric (HF), nitric (HNO3) and hydrochloric (HCl) acid mixture according to SS EN 13656:2003, while another was subject to solubilization through lithium metaborate (LiBO2) fusion according to ASTM D4503: 2008. All samples were subsequently analyzed by inductive coupled plasma mass spectrometry (ICP-MS) for 45 different elements and the results from the method with the highest recovery were reported. For Cu and Zn, the results from the acid digestion were reported. Six paints (P8, P9, P11, P17, P18 and P20) were extracted and analyzed for Cu and Zn in triplicate in order to get an estimate of the analytical error. All samples were also analyzed for loss on ignition (LOI) at 1000 °C as a proxy for the content of organic matter and carbon in the samples.

Table 1
Coatings analyzed for total elements (P1 – P20) and as validation samples by XRF (V1 – V4). Information on the Cu_2O-content as claimed by the manufacturers was obtained from the Swedish Chemical Agency's pesticide register. Paints marked with an asterisk (*) were selected to make standards.

Paint	Type	Manufacturer	Product name	Color	Cu_2O (%)
P1*	Antifouling (amateur use)	International	Cruiser One	Black	8.5
P2*	Antifouling (amateur use)	International	Cruiser One	Red	8.5
P3	Antifouling (amateur use)	International	Cruiser One	Navy	8.5
P4*	Antifouling (amateur use)	International	Cruiser One	Off white	8.5
P5	Antifouling (amateur use)	International	Micron Superior	Navy	31.93
P6	Antifouling (amateur use)	International	Micron Superior	Red	31.93
P7	Antifouling (amateur use)	International	Micron Superior	Off-white	31.93
P8*	Antifouling (amateur use)	Hempel	Mille Light Copper	Red	6.1
P9*	Antifouling (amateur use)	Hempel	Mille Light Copper	Dove white	6.1
P10	Antifouling (amateur use)	Hempel	Hard Racing Xtra	Red	33.1
P11*	Antifouling (amateur use)	Hempel	Mille Xtra	Dove white	34.6
P12	Antifouling (amateur use)	Hempel	Mille Xtra	Red	34.6
P13*	Antifouling (amateur use)	Jotun	NonStop EC	Black	7.0
P14	Antifouling (amateur use)	Jotun	NonStop EC	White	7.0
P15	Antifouling (amateur use)	Jotun	NonStop VK	Black	22.0
P16	Antifouling (amateur use)	Jotun	NonStop VK	White	22.0
P17*	Antifouling (amateur use)	Jotun	Racing VK	Red	22.02
P18*	Antifouling (amateur use)	Jotun	WaterShield	Black	–
P19	Antifouling (professional use)	Jotun	Jotun Seaforce 60 (SPL)	Dark red	31.6
P20*	Antifouling (professional use)	PPG	Sigma Ecofleet 530	Redbrown	39.02
P21	Primer (amateur use)	Hempel	Underwater Primer	Aluminium	–
V1	Antifouling (amateur use)	Biltema	Antifouling BS	Black	7.5
V2	Antifouling (amateur use)	International	Cruiser One	Black	8.5
V3	Antifouling (professional use)	PPG	Sigmarine 290	Redbrown	37.1
V4	Antifouling (professional use)	International	Interspeed 5617	Black	40.0

2.2. Preparation of standards

2.2.1. Paint film preparation and critical thickness

Ten paints (marked with an asterisk in Table 1) were used for the preparation of paint films of varying thicknesses to yield individual calibration curves for each paint. Any potential effect due to differences in absorptive properties could thus be assessed through the comparison of their calibration slopes, i.e. the relationship between the Kα peak areas and the element concentration. The paints were selected to cover a wide range of Cu and Zn concentrations whilst allowing for the assessment of certain specific additives found in high concentrations in the 21 analyzed paints.

In previous studies, different coatings were produced through the

mixing of a generic antifouling paint base with varying additions of Cu_2O and ZnO. Standards with a fixed wet film thickness (WFT) of 100 μm were subsequently produced from these coatings and used to obtain a calibration curve for the XRF analysis [7]. Here, the variation in concentration was instead obtained by producing standards of varying thicknesses for each of the ten paint. Eight different WFTs were used for each paint: 60, 90, 100, 120, 150, 200, 300 and 400 μm. The paints were applied onto 23 μm thick plastic Mylar® film sheets (Pütz Folien, Germany). The Mylar® film thickness was chosen to be as thin as possible, without being impractical to handle. To obtain smooth paint films, an automatic, motorized film applicator (TQC AB3120) was used. With ten paints and eight WFTs, 80 paint films in total were produced.

The d_{thin} for Cu and Zn was determined for all coatings based on the relationship between XRF-signal (Kα peak area) and DFT in order to include only paint films with thicknesses $\leq d_{thin}$ in the calibration. One measurement point per film was selected for XRF and DFT measurement. The DFT was determined by averaging 5 measurements within that point with a film thickness gauge (Defelsko Positector 6000). For the XRF analysis, triplicate measurements were performed (see 2.3. for details about the XRF instrumentation and spectra processing). Curves between the Cu and Zn Kα peak areas and the DFT were established. All data points were fitted to a polynomial curve of the second degree, whereas linear regression curves were fitted to data points with a DFT <40 μm. The critical thickness, d_{thin}, was calculated as the thickness at which 1% attenuation was observed between the fitted linear and polynomial curves [15,21].

2.2.2. Mounting of standards and calculation of their concentrations

A hollow punch tool was used to punch out circular discs in triplicate from the paint films. Despite the use of the motorized film applicator, it is not possible to produce paint films of complete homogenous thickness across the whole film. Prior to punching, the homogeneity of the films was therefore assessed visually with the aid of a light table and the most homogenous areas suitable for producing standard discs were identified. Blanks consisting of discs of the 23 μm Mylar® film used as substrate for the paint films were also produced. On the XRF instrument used in the current study (Delta-50, Innov-X, Olympus), measurements can be performed with a beam size of either around Ø 3 or 10 mm. As a higher number of counts is desirable for a more accurate analysis, the beam size of 10 mm was used. A punch diameter of 13 mm was selected for the standards as it was evaluated to be the smallest diameter that was still sufficiently large to cover the whole spot size of the X-ray beam with some margin. The average area of paint film produced by the punching tool was determined by producing 10 replicate paper discs and scanning them into a graphic software to determine their exact areas. The relative standard deviation (RSD) of the average punched area was found to be very small at 0.3%. All discs were weighed to a precision of 0.01 mg and the weight of the paint was derived by correcting for the added weight of the underlying Mylar® film. The results from the chemical analysis (C_{paint}, in μg g^{-1}, determined for the very same aliquot of paint as was used to produce the discs), the weight (m, in g) and the average area (A, in cm^2) were then used to calculate the area concentration (C_{area}, in μg cm^{-2}) of Cu and Zn for each disc using the following equation:

$$C_{area} = \frac{C_{paint} \times m}{A} \quad (1)$$

For the XRF analysis to provide accurate data, standards should be as similar as possible to samples. Calibration standards should therefore be measured against the same background/paint substrate as samples. For static field tests, antifouling coatings are typically applied to panels of various types of plastic or steel pre-coated with primer. For the standards to be flexible and allow measurement against any type of background, a solution with XRF sample cup holders was devised. The setup involved securing the painted discs between two Mylar® films, suspended across the opening of a double open-ended XRF sample cup (1000 series, TrimLess® sleeve sample cups, Chemplex, USA). During analysis, the XRF sample cup is oriented with the film-side facing the XRF analyzer window. A piece of background panel of choice (e.g. steel, plastic) can then be placed inside the cup, on top of the mounted paint disc (Fig. 2). The Mylar® film facing the XRF had a thickness of 6 μm, while the film facing the background panel had a thickness of 2.5 μm. It was verified that the Mylar® film over the surface of the paint did not affect the XRF measurement.

2.3. XRF measurements

2.3.1. XRF instrumentation and spectra processing

A portable Delta-50 XRF instrument (Innov-X, Olympus) was used in this study (see Table 2 for instrument specifications). Measurements were performed with the instrument mounted in its test stand, analyzer window facing up. This Delta-50 instrument has already been calibrated and used for the measurement of Cu and Zn in μg/cm^2 in antifouling paints previously (Ytreberg et al., 2017; Lagerström et al., 2018), utilizing the instrument's Empirical Mode where custom calibration curves may be stored. The option to make empirical calibrations is however not a general feature of all portable XRF instruments. To make this method available to a wider range of brands and models, the Empirical Mode was therefore not used here. Instead, the raw spectra were exported as CSV-files, and peak area integration and quantification carried out independently of the instrument software. For simplicity, the default settings used by the instrument for the pre-installed Soil Mode were used for measurement and spectra acquisition, as such a mode is generally available from portable XRF manufacturers and installed on most XRF units. The configuration of the Soil Mode may however differ between instruments. On the Delta-50, the Soil Mode utilizes 3 beams, 15, 40 and 50 kV, for the quantification of different elements. Only X-rays with an energy greater than the binding energy of electrons will be able to expel electrons from a given atom sub-shell (K, L or M). For the generation of Cu and Zn Kα emission lines, the minimum required energy is 8.05 and 8.63 keV, respectively. The optimum operating voltage for measuring should be 2–3 times this energy, i.e. approximately 18–26 kV. The intensities of Cu and Zn Kα peaks are roughly 4-fold with the 40 kV beam compared to the 50 kV beam, mainly due to different filters being used for the 40 kV (2000 μm aluminium filter) and 50 kV (150 μm copper filter) beams. The spectra from the 40 kV beam in Soil Mode were therefore used. All measurements were performed in triplicate. Three paint standards holding low (~200 μg/cm^2), medium (~800 μg/cm^2)

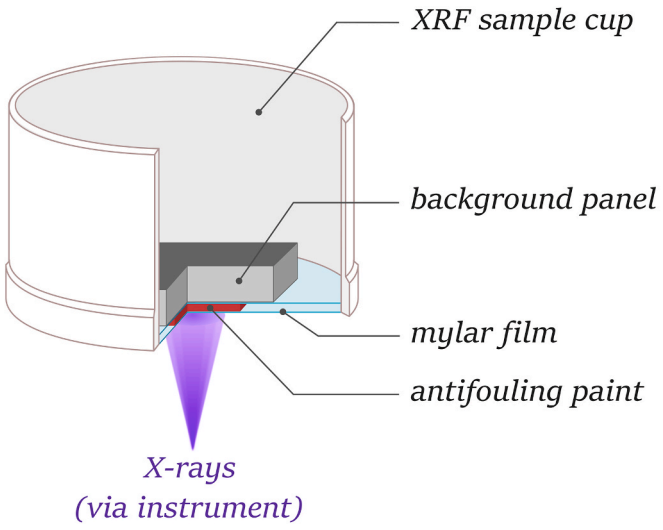

Fig. 2. Schematic of XRF sample cup setup. The antifouling paint disc is here suspended between two Mylar® films across the opening of the cell. A background panel is placed on top of the film. Measurement is performed with the film-side of the sample cup facing the X-ray source.

Table 2
Specifications for the portable XRF instruments used in this study.

Parameter	Innov-X Delta-50	Niton™ XL3t GOLDD+
Manufacturer	Olympus	Thermo Fischer Scientific
Tube type	Ta anode, 50 kV/200 μA	Ag anode, 50 kV/200 μA
Detector	Silicone drift detector	Silicone drift detector
Resolution (eV)	220	150
Beam diameter (mm)	3 or 10	3 or 8
Soil Mode beams/filters	Beam 1 (50 kV/35 μA) Beam 2 (40 kV/36 μA) Beam 3 (15 kV/28 μA)	Main Range (50kV/40 μA) Low Range (20 kV/100 μA) High Range (50kV/40 μA)
Optimum setting for Cu and Zn	Beam 2	Main Range

and high (~2000 μg/cm^2) concentrations of Cu and Zn were measured every 12th sample in order to monitor for instrumental drift. The raw spectra were exported from the instrument for processing in MATLAB where the peaks were subtracted for background, defined as the average signal on either side of the peak, and their areas integrated and normalized to the background scatter. The following integration limits were used: 7.85–8.25 keV for Cu Kα, 8.44–8.66 keV for Zn Kα and 20.3–20.8 keV for the background scatter (see fig. SI3 for an example spectra).

2.3.2. Measurement time

In order to determine an appropriate measurement time for the Delta-50 instrument, various analysis times (10, 15, 20, 30, 45 and 60 s) were evaluated. Two standard cups with paint films holding a high (P20) and a low (P2) copper content were individually analyzed for each different measurement time in random order. Each analysis time was tested five times in total. The difference in precision for each measurement time was evaluated through comparison of the RSDs.

2.3.3. Calibration curves with a plastic background

For this calibration, the background panel consisted of a 2 × 2 cm piece of plastic PVC (Poly Vinyl Chloride, 2 mm thick), coated with primer (paint P21, verified to not contain measurable concentrations of Cu or Zn by XRF) using the motorized film applicator with a WFT of 100 μm. The background panel was placed into the XRF sample cups prior to measurement. As the thin PVC panel consists of light material through which the X-rays can penetrate beyond, an additional piece of plexiglass was placed on top of the background panel in the XRF cup during measurement. The added plexiglass, measured beforehand to ensure the absence of any heavy elements, is used to minimize variations in the scatter peak by ensuring that the total sample thickness was above the saturation thickness of the higher X-rays where the background scatter occurs (>20 keV). A simple test was performed whereby measurements on a sample were carried out with stepwise 2 mm increases in the thickness of the plexiglass. The results showed an increase in background scatter intensity up until a thickness of 14 mm plexiglass was attained. A 16 mm thick plexiglass piece was ultimately used and placed behind all paints in the XRF cups during XRF analysis. Calibration curves for each individual paint (n = 10) were established based on linear regressions between the calculated area concentrations (equation (1)) and the average XRF Kα peak area (n = 3) for each standard disc. An overall universal/generic calibration curve, including the standards produced from all the different paints, was also established. To evaluate differences in slope, potentially due to variations in paint matrix, an analysis of means (ANOM) was performed whereby each slope is tested for significant difference compared to the overall mean slope (significance level of 5%, JMP Pro 15).

2.3.4. Validation

Any new analytical method should be validated through measurements of certified materials or through comparison with a standard method. Although there are some certified materials for the measurement of Pb in paint films, no such materials exist to enable the validation of measurements of Cu or Zn by XRF. To test the performance of the generated calibration, a set of independent validation samples were measured as unknowns. These consisted of paint films of four different commercial antifouling paints, designated V1 – V4 (Table 1). These films (WFT ≤ 100 μm) were produced in 2016 and 2017 as part of other studies and chemically analyzed at those times for Cu and Zn according to the same standard method described previously. Even though paint V2 is also included in this study (P1 of Table 1), the validation samples were generated from a separate batch of the paint obtained during a previous year. The validation samples (n = 14) were mounted in sample cups and measured by XRF following the same procedure as the calibration standards. The concentration range of the validation samples were within those of the calibration curves for Cu and Zn. Linear regressions were established for Cu and Zn between the concentrations determined by the chemical analysis and by XRF. Criteria outlined by the US EPA and developed for comparison between XRF and wet chemical methods for soil samples were then utilized to assess the level of the data quality [27]. According to these, if 1) the coefficient of correlation (r^2) is > 0.85, 2) the regression slope and intercept statistically equivalent to 1 and 0, respectively (significance level of 5%), and 3) the precision (measured as RSD) is below 10%, the XRF can be considered to produce definitive level data.

2.3.5. Transferability – other background materials and instruments

To investigate how the background material of the panel may impact the quantification, the same procedures for calibration and validation used for the plastic background were followed but with a steel background. For this calibration, the background panel consisted of a 2 × 2 cm piece of the type of steel used for ship hulls (Normal Strength Steel, 5 mm). Additionally, the procedures for calibration and validation with the plastic background were also repeated on an XRF instrument of a different brand to assess the transferability of the method and to compare the results between the two instruments. Measurements were performed on a Niton™ XL3t GOLDD + XRF Analyzer using its pre-installed Soil Mode (see Table 2 for specifications). In the Soil Mode, two beam energies are utilized across three filters labeled as the "Main Range" (50 kV), "Low Range" (20 kV) and "High Range" filters (50 kV). According to the Niton instrument manual, the Main range filter is designed to provide optimum sensitivity for the elements of manganese through bismuth. Measurements of the standards were thus performed in the instrument's test stand using this setting. Analyses were performed in triplicate with a beam diameter of 8 mm and a measurement time of 20 s was used. The raw spectra were exported for peak integration in MATLAB following the procedure previously described. The Compton peak from the Ta target of the X-Ray tube on the Delta-50 instrument is not visible in the spectra as the beam filter blocks it out. Scatter correction can therefore only be performed using the background-ratio approach. On the Niton instrument, however, the Ag anode yields a clear Compton peak which could be used for normalization. Two types of scatter normalization were tested: background-ratio and Compton-ratio. The background scatter was integrated between 30.6 and 31.4 keV to not overlap with the Ag Compton peak (integrated between 19.8 and 21.4 keV).

3. Results & discussion

3.1. Paint composition

In total, 21 paints were analyzed for 45 elements as well as loss on ignition (LOI) (see the Supporting Information for all analysis results). The results in Table 3 show that the elemental analysis was able to

Table 3
Elemental composition of the 21 analyzed paints. All concentrations are in percentage of the total dry weight. Concentrations <1 wt % have been marked as "-". Paints marked with an asterisk (*) were selected to make standards.

Paint	Color	Identified composition (%)	Σ LOI and light elements (%)	Heavy elements >1 wt % in any sample (%)									Σ remaining heavy elements (%)
				Mg	Al	Si	S	Ca	Ti	Fe	Cu	Zn	
P1*	Black	85	48	2	–	3	–	–	–	–	9	23	–
P2*	Red	82	39	2	–	4	–	–	–	9	8	20	–
P3	Navy	83	43	2	–	4	–	–	–	–	10	25	–
P4*	Off white	81	37	1	–	3	–	–	7	–	9	23	–
P5	Navy	79	30	–	–	–	3	4	–	–	30	10	–
P6	Red	80	30	–	–	–	3	4	–	3	30	9	–
P7	Off-white	76	26	–	–	–	3	3	8	–	26	9	–
P8*	Red	80	46	3	1	4	–	5	–	1	8	11	–
P9*	Dove white	79	42	3	1	4	–	4	6	–	8	11	–
P10	Red	80	23	–	–	2	–	–	–	–	36	16	–
P11*	Dove white	77	26	–	–	–	–	1	6	–	35	8	–
P12	Red	75	26	–	–	2	–	–	–	–	37	8	–
P13*	Black	81	39	3	–	–	–	2	–	–	8	26	–
P14	White	84	33	3	–	2	–	2	10	–	8	25	–
P15	Black	82	32	2	–	–	–	3	–	–	24	21	–
P16	White	89	38	–	–	–	8	–	9	–	15	20	–
P17*	Red	78	27	–	–	–	–	1	–	–	25	24	–
P18*	Black	84	64	6	1	6	–	2	–	–	–	4	–
P19	Dark red	77	21	–	–	–	–	–	–	2	35	16	–
P20*	Redbrown	80	24	–	–	1	–	–	–	4	38	11	–
P21	Aluminium	76	46	2	10	2	–	15	–	–	–	–	–

account for the majority (75–89 wt %) of the composition of the dry paints. The chemical composition data was processed in two steps. Firstly, the content of elements too light to be detected by XRF (LOI and all elements < Mg) were summed together. In a second step, only the remaining heavy elements constituting ≥1% of the total dry weight in any sample were considered whereas the rest were summed together.

Out of all the XRF detectable elements, nine were present at concentrations ≥ 1 wt % in one or more of the 21 samples: Mg, Al, Si, S, Ca, Ti, Fe, Cu and Zn. By far, the most abundant heavy elements in the paints were Cu (8–40 wt %) and Zn (8–26 wt %). As to be expected, exceptions to this are the primer (P21) (where both Cu and Zn are < 0.1 wt %) and the freshwater paint (P18) which did not contain any added Cu_2O. Also found in notable concentrations in many of the paints are Ti and Fe whose presence appear to be related to the color of the paints. Ti is found in concentrations ≥1 wt % exclusively in products of white color, suggesting TiO_2 has been added as a white pigment to these paints. Fe ≥ 1 wt %, on the other hand, is only found in products of red color, probably due to the addition of the red pigment Fe_2O_3 to their formulations. A red pigment other than Fe_2O_3 must however have been added to the red paint P17 as Fe was <0.1 wt %. The presence of Mg, Al, Si, S and Ca in many of the paints likely reflect the composition of the fillers and extenders added to the paints such as calcium sulphate, calcium carbonate and various silicates such as silica, talc (i.e. magnesium silicate) and mica (i.e. aluminium silicate) [26].

As previously mentioned, XRF analysis can be subject to both absorption and enhancement effects. The origin of these effects may be general (non-specific) or specific. The former involves only absorption effects and result from differences in the ability of the analyte and matrix element to absorb primary and secondary X-Rays. Specific enhancement or absorption effects are, on the other hand, caused by individual elements in the matrix [17]. With knowledge of the composition of antifouling paints, such effects can be investigated. The minimum photon energy needed to expel an electron from a given sub-shell for an element is known as the absorption edge. For a given analyte however, its signal will be highly absorbed by elements with absorption edges at energies just below that of the analyte's characteristic line energy. Conversely, if the energy of the absorption edge of the analyte is just below the energy of the characteristic line of a matrix element, the intensity of the analyte signal will be enhanced by that element. Ultimately, the extent of any of these specific effects will depend on the proximity of spectral lines and absorption edges of analyte and matrix elements [17]. For the analytes Cu (Kα-line at 8.04 keV) and Zn (Kα-line at 8.64 keV), the energy range of concern in the spectra is between 7 and 10 keV. Since Mg, Al, Si, S, Ca and Ti have characteristic lines and absorption edges <5 keV, these elements are not likely to impact the signals of Cu or Zn. Fe could however potentially exert specific absorption effects as its absorption edge is at 7.11 keV, i.e. at an energy below both the Cu and Zn Kα lines (Fig. 3). Even so, such effects are likely limited as the absorption edge sits somewhat away from the Cu Kα line, and even further from the Zn Kα line. Finally, possible effects can be caused by the two principal heavy elements in the analyzed antifouling paints: Cu and Zn themselves. The absorption edges of Cu (8.98 keV) and Zn (9.66 keV) are above the characteristic Kα lines of both elements as well as the Cu Kβ line (8.91 keV). The Zn Kβ line (9.57 keV) is however above the Cu K edge and may thus cause enhancement of the Cu signal at the expense of the intensity of the Zn Kβ signal. Potential effects of Fe (absorption of Cu and Zn) and Zn (enhancement of Cu) on the measured peak areas will be assessed and discussed further in the next section.

3.2. Calibration curves with a plastic background

3.2.1. Measurement time

Prior to any measurement on the XRF, an evaluation to determine an appropriate measurement time was carried out. The results from the test of six different measurement times between 10 and 60 s show similar results for both tested paints (P2 and P20) (fig. SI1). The lowest precision (highest RSD, ~1%) was obtained for the shortest measurement time of 10 s. The precision improves when the measurement time is

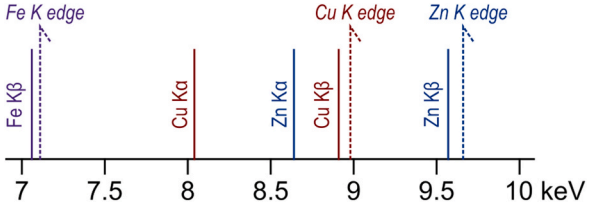

Fig. 3. Absorption edges (dashed lines) and characteristic lines (full lines) of matrix elements that may cause specific absorption/enhancement effect on the analytes Cu and Zn.

increased to 15 s (~0.7%) and even further when analyzing for 20 s (~0.4%). No clear improvement in precision is however obtained when increasing the measurement time beyond 20 s. These results therefore indicate that a measurement time of 20 s should be used for the highest quality analysis in the least amount of time.

3.2.2. Comparison of slopes

The critical thickness was determined for the 10 selected paints (data not shown) so that only paint films of thicknesses within the linear range were included in the regression curves. All films produced with a WFT of 100 μm were found to be within the linear range for all paints. Additionally, for some of the paints with lower amounts of Cu, WFTs of up to 150 μm were inside the linear range and could thus be included. 10 standard series with triplicate discs for each WFT were thus produced, mounted in XRF cups and measured by XRF along with the blanks. Upon determination of the scatter normalized Cu and Zn Kα peak areas, individual linear regression curves were established for each paint as well as an overall regression curve based on the data points from all the paints. The overall regressions curves are shown in Fig. 4 and regression parameters are outlined in Table SI2. All individual regressions were found to be significant for both Cu and Zn ($p < 0.0001$) and the majority hold r^2-values ≥ 0.99 or better. The individual slopes range between 7.1–8.1 $\times 10^{-3}$ for Cu and between 5.0–5.9 $\times 10^{-3}$for Zn. To test for significant differences in slope, an ANOM was performed whereby each paint's slope was compared to the overall mean slope (the ANOM results are outlined in Tables SI3 and SI4 of the Supplementary Information). For Cu, one slope (P11) was found to be significantly above the overall mean slope. For Zn, the slope of P11 was found to be significantly below the overall mean slope while P17 was found to be significantly above. These discrepancies can be explained by either matrix effects and/or uncertainties in the chemical analysis and are discussed further below.

The normalization of the Kα peak areas to the background scatter in each respective XRF spectra should, in principle, compensate for matrix effects as well as aid in correcting for any short-term (e.g. detector drift) and long-term drift (e.g. ware of the X-Ray tube). The drift here, as monitored through the precision of repeated measurements of three standards, was found to be small. The RSD of the three drift standards was however slightly improved from an average of 1.0%–0.3% when the scatter normalization was applied. Of greater importance, the scatter normalization reduced the RSD of the individual slopes from 17.4 to 4.5% for Cu and from 20.1 to 4.9% for Zn (Fig. 5). The magnitude of this change is far greater than that of the drift (<1%). Hence, the bulk of the reduction in slope variability is likely the result of matrix effect correction. As scatter methods are generally not able to compensate for enhancement effects, mainly absorption effects may be attenuated through the use of the background-ratio method [17]. As discussed previously, Fe may cause absorption effects firstly on Cu and secondly on Zn. Such an effect would result in lower slopes for paints containing Fe. Three of the paints (P2, P8 and P20) hold Fe concentrations > 1 wt % but these show no overall tendency to hold lower slopes compared to the other paints (Table SI2). Furthermore, direct comparison of the slopes of paints P2 (9% Fe) and P1 (0.2% Fe) which have different amount of Fe but otherwise nearly identical compositions, reveals no significant difference in slope either. Enhancement of the Cu signal by Zn Kβ was also identified as a potential specific effect. However, plotting the chemically determined Cu:Zn ratios against the measured Cu Kα:Zn Kα reveals a significant linear relationship ($r^2 = 0.999$, $p < 0.0001$) (fig. SI2). This result indicates that variations in the Zn content of the antifouling paints does not bias the measurement of Cu by XRF.

As for all empirical XRF methods, the quality of the calibration depends on that of its standards. First and foremost, it is important that the paints used for standards are properly homogenized prior to the production of the paint films. The degree of homogenization here can be inferred from the RSD of the Cu Kα:Zn Kα ratios which was on average of

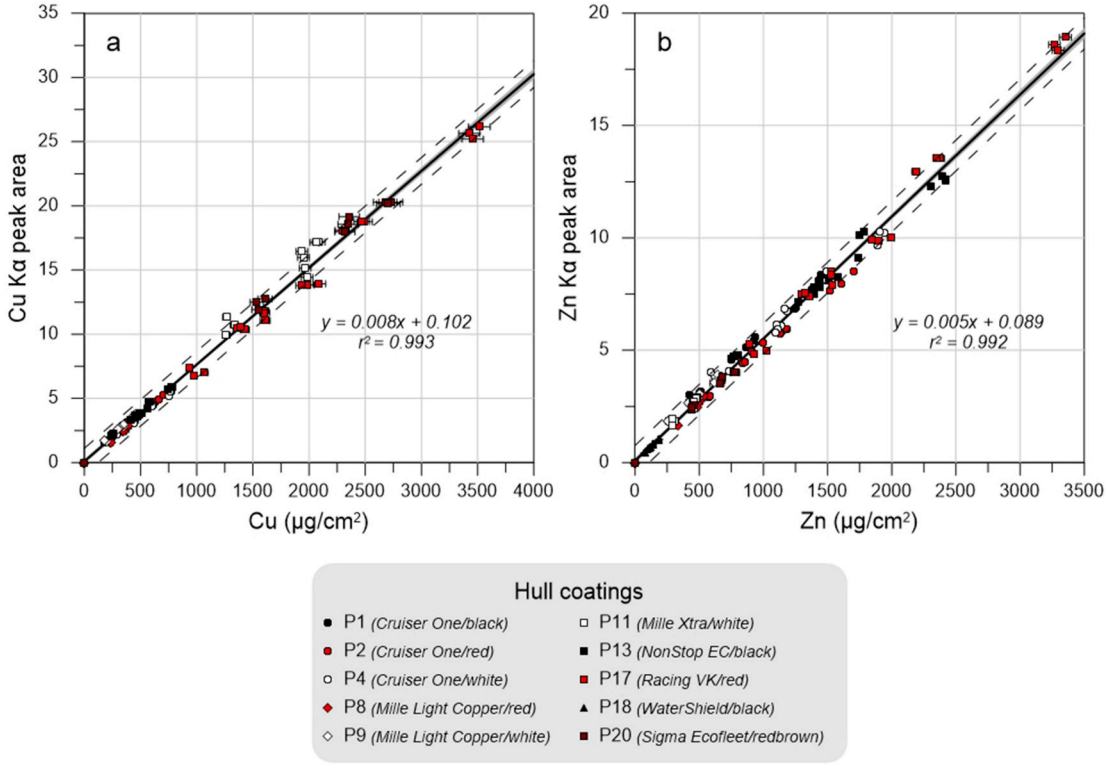

Fig. 4. Linear regression curves between Kα peak areas (scatter normalized) and area concentrations based on ten coatings for Cu (a) and Zn (b). Vertical error bars show the standard deviation of triplicate XRF measurements. Horizontal error bars show the total range (minimum and maximum) of the estimated area concentration of triplicate chemical analyses performed on six of the paints (see 2.1). The shaded grey area on either side of the overall linear regression (solid line) shows the 95% confidence intervals of the slopes. Note that these are small and thus may be difficult to see. The dashed lines show the 95% prediction interval.

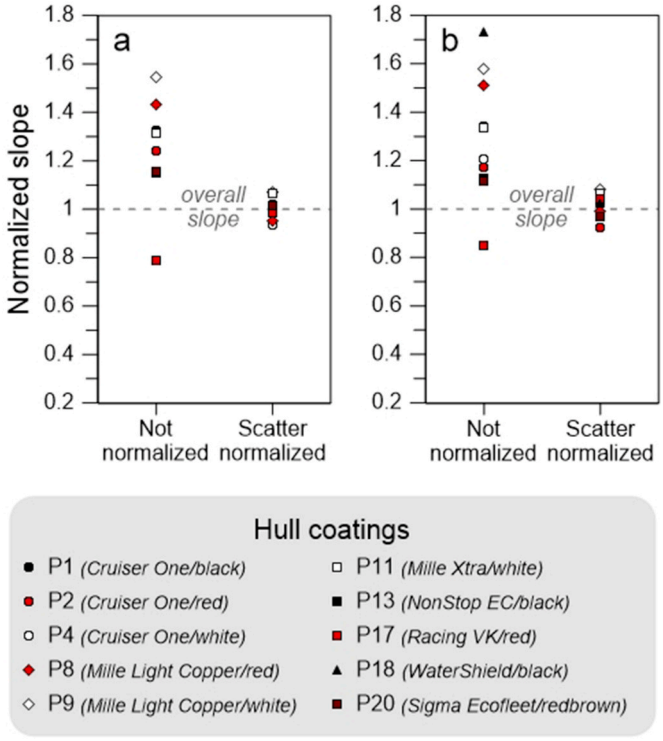

Fig. 5. Distribution of individual slopes for Cu (a) and Zn (b) with and without background scatter normalization of the peak areas. The slopes have been normalized to their respective overall slope (i.e. the slope based on the data points of all paints). A slope of "1" is thus equal to the overall slope. The blue error bar shows the magnitude of the precision (±5.5%) of the chemical analysis. (For interpretation of the references to color in this figure legend, the reader is referred to the Web version of this article.)

1.2% (0.4–3.1%, depending on the paint), suggesting the paints were indeed properly mixed before painting. As the sub-samples for the chemical analysis were taken from the exact aliquots used to produce the paint films, the homogeneity of both standards and chemically analyzed paint samples can be assumed similar. The concentrations in the standards are determined from their area, weight and metal content (Equation (1)). Errors associated with the weight and area determinations are expected to be small. Uncertainties in the chemical analysis are thus the only remaining source of error. The accuracy of the chemical analysis is of utmost importance as the analysis results have direct bearing on the slope estimates. An overall increase of all area concentrations by 5%, for example, equals a 5% decrease of the overall slope estimate. Triplicate chemical analyses were carried out for six of the ten paints, enabling an estimation of the laboratory precision. An average RSD of 5.5% was calculated for both Cu and Zn (illustrated by the blue error bar in Fig. 5). The magnitude of this uncertainty is directly comparable with that of the variation between the individual Cu and Zn slopes (4.5% and 4.9%, respectively). Indeed, when only the highest reported concentrations for Cu from the chemical analysis was used to determine the area concentrations of the P11 standards, the P11 slope was no longer found to be significantly different from the overall mean slope when repeating the ANOM. The observed variation in slope may thus be due to some residual matrix effects for which the scatter normalization was unable to compensate for and/or the uncertainties of the chemical analysis, such as small variations in the recovery of the acid digestion. The laboratory method employed here for the extraction of Cu and Zn from the dried paint samples was a microwave assisted acid digestion with a mixture of HNO_3, HCl and HF. Although full decomposition of paint samples through wet digestion techniques is not an easy task, the combined use of the above-mentioned acids should have aided to solubilize the paint samples as completely as possible [28]. Nonetheless, regardless of metal, all the individual slopes' 95% confidence interval overlap with those of at least three other slopes (Table SI2). Given the uncertainty of the chemical analysis, the most accurate quantification of unknown samples will be obtained when the overall regression based on all paints is used as the calibration curve. The data points included in this universal antifouling paint calibration then originate from the chemical analysis of ten different paints generated from a total of 22 extractions. For the overall regressions, the uncertainty of any singular predicted value with a primed PVC panel background, as derived from the 95% prediction interval of the linear regressions, are ±136 μg/cm^2 for Cu and ±125 μg/cm^2 for Zn.

3.2.3. Validation

The chemically determined concentrations of Cu and Zn in the validation samples are plotted against those determined by XRF in Fig. 6 and show very good overall agreement between the two methods. Root mean square errors were 164 μg/cm^2 for Cu and 50 μg/cm^2 for Zn.

To assess the quality level of the XRF data according to the US EPA criteria, analysis of the regression parameters and the precision was performed. The precision of the triplicate measurements was well below the 10% criteria for both Cu and Zn, with calculated RSDs ≤2%. The regressions of Cu and Zn were both found to be significant ($p < 0.0001$) and hold respective r^2-values of 0.976 and 0.989, thus above the 0.85 criteria. For Cu, the slope (95% confidence interval: 0.91–1.11) and intercept (95% confidence interval: 126 – 212) were determined to not be significantly different compared to 1 and 0, respectively. Thus, the two data sets can be considered statistically similar, meeting all the criteria for definitive level. This was however not the case for Zn, where both the slope (95% confidence interval: 1.10–1.26) and intercept (95% confidence interval: 153 to −15) were significantly different from 1 to 0, respectively. This offset appears to be driven by the result of the samples from paint V1, which act to increase the slope of the regression line (Fig. 6b). For these samples, the XRF measurement predicted higher Zn concentrations than those determined chemically. It is not uncommon for XRF analyses to show higher concentrations than those determined through wet chemical methods, given that the latter is dependent on full solubilization of the sample, as discussed previously. When excluding the V1 samples, the confidence intervals of both the slope (0.96–1.19) and intercept (-110 – 45.6) meet the definitive level criteria.

3.2.4. Transferability – other backgrounds and instruments

The same procedure for calibration and validation was repeated on the Delta-50 instrument but with a steel background. The steel background calibration on the Delta-50 analyzer could only be performed for Cu as the steel panel contained a high and variable concentration of Zn in itself. This introduced noise into the Zn data set, resulting in a very poor calibration curve ($r^2 < 0.9$). As seen in Table 4, all parameters for Cu (e.g. r^2-value, prediction interval and recovery of validation samples) were poorer with the steel background compared to those obtained using the plastic background. Additionally, fewer standards could be included in the calibration as the linear range was found to be narrower. Although the variation in slope between individual paints was reduced upon normalization, the remaining variation was still large, 8.9%. With the steel background, the concentration of light elements in the measured standards is lower than with the plastic background, resulting in a roughly five times lower background scatter signal. Additionally, the variation in background scatter between paints was also reduced by half and thus less sensitive to variations in matrix. The inferior performance with the steel background is therefore likely due to the background-ratio normalization being unable to successfully compensate for matrix effects. Consequently, a universal calibration curve using the steel background will not yield the most accurate results. Paint-specific calibrations could however still be established, if a steel background is desired.

Given the inferior results with the steel panel, the plastic background was used for the tests on the Niton instrument. Examples of spectra from

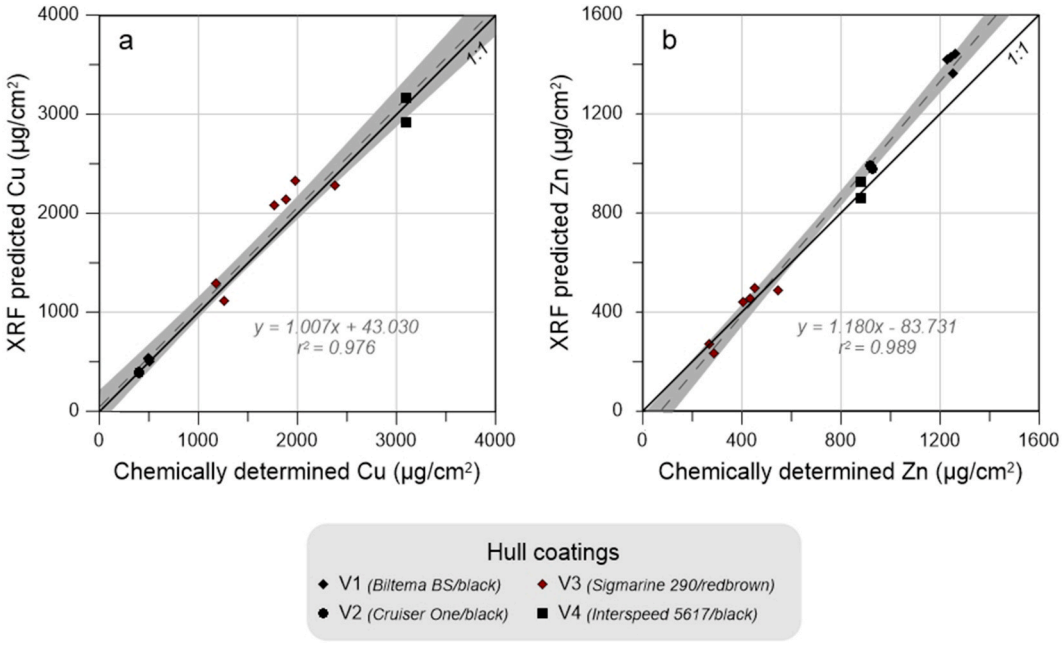

Fig. 6. Chemically determined versus XRF determined concentrations for Cu (a) and Zn (b). Error bars (although too small to be visible) show the standard deviation of triplicate XRF determinations. The solid line shows the 1:1 correlation whereas the dashed grey line shows the linear regression line of the data. The 95% confidence interval of the regression slope is also shown (shaded area).

Table 4
Compiled results of different calibrations on the two instruments.

		Delta-50 (40 kV, 10 mm beam diameter)		Niton (50 kV, 8 mm beam diameter)	
Background panel		Plastic	Steel	Plastic	Plastic
Normalization type (integration interval)		Background-ratio (20.3–20.8 keV)	Background-ratio (20.3–20.8 keV)	Background-ratio (30.6–31.4 keV)	Compton-ratio (19.8–21.4 keV)
Variation between individual paint slopes (RSD in %)	Cu	4.5	8.9	6.4	5.1
	Zn	4.9	n/a	6.7	6.4
r^2 of overall regression curve and number of data points	Cu	0.993 (n = 119)	0.986 (n = 99) n/a	0.993 (n = 108)	0.998 (n = 128)
	Zn	0.992 (n = 133)		0.991 (n = 122)	0.990 (n = 142)
95% prediction interval (µg/cm^2)	Cu	±136	±425	±139	±116
	Zn	±125	n/a	±113	±139
Average recovery of validation samples ± 1 standard deviation (%)	Cu	104 ± 9	90 ± 12	101 ± 7	97 ± 7
	Zn	105 ± 10	n/a	97 ± 12	98 ± 7

the two instruments for the same sample are shown in figure SI3. As a higher energy (50 kV) is used by the Niton instrument, a lower background (fig. SI3a) but also lower peak heights (fig. SI3b) are obtained. However, upon normalization to background scatter, peaks of similar magnitude are obtained. The linearity of the calibration curve, the magnitude of the prediction interval and the recovery of validation samples obtained with the Niton instrument were found to be comparable to those obtained with the Delta-50 instrument, regardless of normalization method (Table 4). Thus, both the background- and Compton-ratio normalization can be used to obtain reliable measurements by XRF. However, the extent of the linear range, reflected in Table 4 in the number of data points included in the overall regression, was somewhat reduced when applying the background-ratio. Thus, if the latter is used, slightly thinner paint layers (closer to 35 µm, rather than 40 µm) would have to be applied, with regards to both standards and samples. It may be that the energy region of the spectra used for the measurement of the background scatter signal was less optimum than that used for the Delta-50 or that the background signal was lower due to the higher energy (50 kV) and therefore poorer at compensating for matrix effects. For the Niton instrument, normalization with the Ag Compton peak therefore presents as the best approach.

3.2.5. *Possibilities and limitations*

As variations in paint composition were found to not impact the signal of the analyzed Kα peaks, universal antifouling paint calibration curves based on ten paints were established for the determination of Cu and Zn in µg/cm^2 with a plastic panel background. With these calibrations, the XRF method was capable of quantifying Cu and Zn in antifouling paint films both accurately and precisely, with a prediction uncertainty of around ±130 µg/cm^2 and RSDs typically around 1%. Additionally, transferability of the method to another instrument was also confirmed, supporting the possibility for its standardization. Although the XRF method requires an initial investment in specific instrumentation and calibration, these are one-time expenditures as the calibration curve needs to be measured and derived only once. Thereafter, the performance of the instrument can be sufficiently monitored through measurement of dedicated drift standards. The operating costs of the instrument are also low, making the XRF method more cost-effective in the long-term for release rate measurements of Cu and Zn compared to e.g. the rotating cylinder method (Table SI1), which requires 40 chemical analyses of seawater samples per paint and release rate trial [29]. Additionally, as far as analytical techniques are concerned, XRF analyses are relatively simple and easy to perform compared to chemical analyses. The calibrations with different instruments and backgrounds in this study show that it is possible to

accurately quantify Cu and Zn in paint films with ±5% of chemically determined concentrations if an appropriate configuration (e.g. materials, instrument settings and data processing methods) is used. Firstly, to utilize the method, an XRF unit with a voltage capability of at least 40 kV is recommended. Spectra acquisition can be performed with the settings of a pre-installed Soil Mode, as demonstrated for the two instruments in this study, and spectra processing involves simple integration of peak areas which can be carried out in an independent and commonly available software such as Matlab or Excel. Secondly, for the application of a universal/generic antifouling paint calibration, a light background panel material (e.g. plastic) should be used. Finally, scatter normalization should be performed and the type of normalization (background- or Compton-ratio) as well as the extent of the linear range should be evaluated before implementing the method on a new instrument.

A pre-requisite to use the universal calibration curves for the determination of Cu and Zn is that the thickness of the paint sample must be within the linear range, i.e. $\leq d_{thin}$. As mentioned in the introduction, it is only at thicknesses $\leq d_{thin}$ that the concentration in the sample is linearly proportional to the measured peak area. If d_{thin} is exceeded, the full amount of metals present within the measured paint film will not be quantified properly due to signal attenuation effects (Fig. 1). For the obtainment of smooth paint films with a controlled thickness, the use of an automated paint film applicator for the coating application is highly recommended. Determinations of d_{thin} for two antifouling paints in a previous study suggested paint films should be $\leq$ 40 μm [15]. This general recommendation was found to be valid for the majority of the ten paints studied here. The d_{thin} of a specific paint is related to its composition. Here, a DFT of up to 50 μm was found to be within the linear range for Cu for some coatings with low Cu content. Oppositely, a DFT $\leq$30 μm was found to be more appropriate for some coatings with high Cu contents (e.g. Sigma Ecofleet 530). For many antifouling paints, a DFT $\leq$40 μm is typically below that of the recommended for the use of the product on a hull. However, it is important to note that the release rate from the paint is not a function of its thickness, as the interaction between seawater and paint leading to the release of metals from the coating during immersion occurs at the surface of the paint. The thickness will however determine the longevity (lifetime) of the paint as the coating will successively be depleted in copper over time with exposure to seawater. Long-term studies (>2 months) of the release rate can therefore be challenging when using the proposed universal calibration curve. Also important to take into account is that the release rate of Cu (i.e. its depletion rate from the paint film) is greatly affected by salinity, with increased release at higher salinities [7,15,30]. The maximum possible length of the exposure will consequently be a product of both the d_{thin} of the specific paint and the salinity of the exposure location, with longer studies possible for paints with lower copper content and at locations with lower salinities. If studies over longer time periods than these conditions will allow are of interest, it is possible to use thicker paint films and correct for the signal attenuation. By establishing the relationship between signal intensity (i.e. peak area) and DFT for a specific paint (Fig. 1a), attenuation correction factors as a function of the DFT can be derived. Before field exposure, a film thickness gauge could then be used to determine the DFT of the paint film at the XRF measurement point to determine the appropriate attenuation correction factor to be applied to the measured peak area. Due to the formation of a so-called "leached layer" depleted of Cu and Zn at the surface of the paint film upon immersion [10,31], the metals will no longer be uniformly distributed throughout the paint film after exposure. Application of any attenuation correction factor would therefore not be appropriate at this time. For an accurate determination of the metal concentrations after exposure, the DFT will need to be within the linear range. Hence, although the simplest application of the XRF method is for short-term studies of weeks to months, long-term studies are nonetheless also possible.

Funding

This work was supported by the Swedish Agency for Marine and Water Management (SwAM) and the HÅLL project (funded by the Swedish Transport Administration's industry program Sustainable shipping operated by Lighthouse).

Declaration of competing interest

The authors declare that they have no known competing financial interests or personal relationships that could have appeared to influence the work reported in this paper.

Acknowledgements

The authors would like to thank Emma Rova and Felicia Stragnefeldt for their contributions to this study, as well as the Department of Historical Studies at the University of Gothenburg for allowing us the use of their XRF instrument.

Appendix A. Supplementary data

Supplementary data to this article can be found online at https://doi.org/10.1016/j.talanta.2020.121820.

References

[1] E. Almeida, T.C. Diamantino, O. de Sousa, Marine paints: the particular case of antifouling paints, Prog. Org. Coating 59 (2007) 2–20, https://doi.org/10.1016/j.porgcoat.2007.01.017.
[2] R. Edyvean, Consequences of fouling on shipping, in: Biofouling, 2010, pp. 217–225.
[3] WHOI, The history of the prevention of fouling, in: Mar. Fouling its Prev. Annap, US Nav. Inst, 1952, pp. 211–223.
[4] N. Voulvoulis, M.D. Scrimshaw, J.N. Lester, Comparative environmental assessment of biocides used in antifouling paints, Chemosphere 47 (2002) 789–795.
[5] D.M. Yebra, C.E. Weinell, Key issues in the formulation of marine antifouling paints, in: Adv. Mar. Antifouling Coat. Technol., Woodhead Publishing, 2009, pp. 308–333, https://doi.org/10.1533/9781845696313.2.308.
[6] S. Brooks, M. Waldock, 19 - the use of copper as a biocide in marine antifouling paints, in: C. Hellio, D. Yebra (Eds.), Adv. Mar. Antifouling Coat. Technol., Woodhead Publishing, 2009, pp. 492–521, https://doi.org/10.1533/9781845696313.3.492.
[7] M. Lagerström, J.F. Lindgren, A. Holmqvist, M. Dahlström, E. Ytreberg, In situ release rates of Cu and Zn from commercial antifouling paints at different salinities, Mar. Pollut. Bull. 127 (2018) 289–296, https://doi.org/10.1016/j.marpolbul.2017.12.027.
[8] CEPE, Zinc Oxide Use in Antifouling Products, 2011.
[9] European Parliament and Council, Regulation (EU) No 528/2012 of the European Parliament and of the Council of 22 May 2012 Concerning the Making Available on the Market and Use of Biocidal Products, 2012.
[10] D.M. Yebra, S. Kiil, C.E. Weinell, K. Dam-Johansen, Dissolution rate measurements of sea water soluble pigments for antifouling paints: ZnO, Prog. Org. Coating 56 (2006) 327–337, https://doi.org/10.1016/j.porgcoat.2006.06.007.
[11] K. Takahashi, Release rate of biocides from antifouling paints, in: Ecotoxicol. Antifouling Biocides, 2009, pp. 3–22.
[12] K.V. Thomas, S. Brooks, The environmental fate and effects of antifouling paint biocides, Biofouling 26 (2010) 73–88, https://doi.org/10.1080/08927010903216564.
[13] K.A. Dafforn, J.A. Lewis, E.L. Johnston, Antifouling strategies: history and regulation, ecological impacts and mitigation, Mar. Pollut. Bull. 62 (2011) 453–465, https://doi.org/10.1016/j.marpolbul.2011.01.012.
[14] IMO, The generation of biocide leaching rate estimates for anti-fouling coatings and their use in the development of proposals to amend annex 1 of the AFS Convention, MEPC 60/13 (2009).
[15] E. Ytreberg, M. Lagerström, A. Holmqvist, B. Eklund, H. Elwing, M. Dahlström, P. Dahl, M. Dahlström, A novel XRF method to measure environmental release of copper and zinc from antifouling paints, Environ. Pollut. (2017), https://doi.org/10.1016/j.envpol.2017.03.014.
[16] R. DeKosky, Developing chemical instrumentation for environmental use in the late twentieth century: detecting lead in paint using portable X-ray fluorescence spectrometry, Ambix 56 (2009) 138–162.
[17] E.P. Bertin, Principles and Practice of X-Ray Spectrometric Analysis, Plenum Press, 1975.
[18] P.J. Potts, M. West, Portable X-Ray Fluorescence Spectrometry: Capabilities for in Situ Analysis, Royal Society of Chemistry, 2008.

[19] D.C. Weindorf, N. Bakr, Y. Zhu, Chapter one - advances in portable X-ray fluorescence (PXRF) for environmental, pedological, and agronomic applications, in: D.L. Sparks (Ed.), Adv. Agron., Academic Press, 2014, pp. 1–45, https://doi.org/10.1016/B978-0-12-802139-2.00001-9.
[20] R. Jenkins, X-Ray Fluorescence Spectrometry, second ed., John Wiley & Sons, Inc., 1999.
[21] G. Gauglitz, T. Vo-Dinh, Handbook of Spectroscopy, John Wiley & Sons, 2006.
[22] R. Sitko, Quantitative X-ray fluorescence analysis of samples of less than 'infinite thickness': difficulties and possibilities, Spectrochim. Acta Part B At. Spectrosc. 64 (2009) 1161–1172, https://doi.org/10.1016/j.sab.2009.09.005.
[23] A. Markowicz, An overview of quantification methods in energy-dispersive X-ray fluorescence analysis, Pramana 76 (2011) 321–329, https://doi.org/10.1007/s12043-011-0045-z.
[24] R.M. Rousseau, J.P. Willis, A.R. Duncan, Practical XRF calibration procedures for major and trace elements, X Ray Spectrom. 25 (1996) 179–189, https://doi.org/10.1002/(SICI)1097-4539(199607)25:4<179::AID-XRS162>3.0.CO;2-Y.
[25] M. Mantler, J. Willis, G. Lachance, B.A.R. Vrebos, K.-E. Mauser, N. Kawahara, R. M. Rousseau, P.N. Brouwer, Quantitative analysis, in: D.B. Beckhoff, D. habil, B. Kanngießer, P.D.N. Langhoff, D. sc nat R. Wedell, D. sc nat H. Wolff (Eds.), Handb. Pract. X-Ray Fluoresc. Anal., Springer Berlin Heidelberg, 2006, pp. 309–410, https://doi.org/10.1007/978-3-540-36722-2_5.
[26] R. Lambourne, T.A. Strivens, Paint and Surface Coatings: Theory and Practice, 2 edition, Woodhead Publishing, Cambridge, Eng, 1999.
[27] US EPA, Environmental technology verification report: field portable X-ray fluorescence analyzer, Metorex X-MET 920-P and 940 (1998).
[28] F.L.F. Silva, T.A.O. Duarte, L.S. Melo, L.P.D. Ribeiro, S.T. Gouveia, G.S. Lopes, W. O. Matos, Development of a wet digestion method for paints for the determination of metals and metalloids using inductively coupled plasma optical emission spectrometry, Talanta 146 (2016) 188–194, https://doi.org/10.1016/j.talanta.2015.08.040.
[29] ISO, Determination of the release rate of biocides from anti-fouling paints, International Standard ISO 15181 (2007) 2007.
[30] J.D. Ferry, D.E. Carritt, Action of antifouling paints, Ind. Eng. Chem. 38 (1946) 612–617, https://doi.org/10.1021/ie50438a021.
[31] C. Anderson, Coatings, antifoulings, in: Kirk-Othmer Encycl. Chem. Technol., John Wiley & Sons, Inc., 2000.